

VOLUME 79

SEPARATE No. 296

PROCEEDINGS

AMERICAN SOCIETY
OF
CIVIL ENGINEERS

OCTOBER, 1953



AN EXPERIMENTAL INVESTIGATION AND
LIMIT ANALYSIS OF NET AREA
IN TENSION

by W. G. Brady and D. C. Drucker, A.M. ASCE

Presented at
New York City Convention
October 19-22, 1953

ENGINEERING MECHANICS DIVISION

{Discussion open until February 1, 1954}

Copyright 1953 by the AMERICAN SOCIETY OF CIVIL ENGINEERS
Printed in the United States of America

Headquarters of the Society
33 W. 39th St.
New York 18, N. Y.

PRICE \$0.50 PER COPY

THIS PAPER

--represents an effort of the Society to deliver technical data direct from the author to the reader with the greatest possible speed. To this end, it has had none of the usual editing required in more formal publication procedures.

Readers are invited to submit discussion applying to current papers. For this paper the final closing dead line appears on the front cover.

Those who are planning papers or discussions for "Proceedings" will expedite Division and Committee action measurably by first studying "Publication Procedure for Technical Papers" (Proceedings — Separate No. 290). For free copies of this Separate—describing style, content, and format—address the Manager, Technical Publications, ASCE.

Reprints from this publication may be made on condition that the full title of paper, name of author, page reference, and date of publication by the Society are given.

The Society is not responsible for any statement made or opinion expressed in its publications.

This paper was published at 1745 S. State Street, Ann Arbor, Mich., by the American Society of Civil Engineers. Editorial and General Offices are at 33 West Thirty-ninth Street, New York 18, N. Y.

AN EXPERIMENTAL INVESTIGATION AND LIMIT ANALYSIS OF NET AREA IN TENSION*

W. G. Brady** and D. C. Drucker*** (Brown University)

Abstract

The old question of the weakening effect of holes in tension members is re-examined from the viewpoint of plastic action. Using the maximum shearing stress yield criterion and the Mises criterion, upper and lower bounds for the limit load are computed for thin sheets with six configurations of staggered rows of holes. The limit load is defined as the force required for unrestricted flow across the entire member. Comparison is made with current design specifications, and with the results of a large number of tests performed on hot-rolled steel and on 61S-T6 aluminum alloy sheet. Plugs were inserted in the holes in a few of the tests. It is found that the limit loads, as determined by test, confirm the main features of the analysis, and lie somewhat above the ranges of load computed with the maximum shearing stress criterion. The $s^2/4g$ design rule is shown to correspond to an approximate upper bound, and as such, may be appreciably on the unsafe side for configurations of open or plugged holes, although probably reasonable for riveted tension joints.

Introduction

The recently developed theorems for limit analysis^{1,2} offer an opportunity to check current design specifications for net area in tension members, as well as to determine how closely the limit loads of selected configurations of rows of holes in steel and aluminum alloy sheets, as determined by test, agree with idealized theory. The limit load is here defined as the force required for unrestricted plastic flow to occur across the entire section and is therefore above the load at which plastic deformation first occurs. At this stage, either localized or overall plastic deformation is considerable so that the limit load may provide a reasonable value upon which to base the working load.

*The results presented in this paper were obtained in the course of research sponsored by the Office of Naval Research under Contract N7onr 35801.

**Research Assistant in Applied Mathematics.

***Chairman, Division of Engineering.

1. "The Safety Factor of an Elastic-Plastic Body in Plane Strain", by D. C. Drucker, H. J. Greenberg, and W. Prager, Journal of Applied Mechanics, vol. 18, 1951, pp. 371-378.
2. "Extended Limit Design Theorems for Continuous Media", by D. C. Drucker, W. Prager, and H. J. Greenberg, Quarterly of Applied Mathematics, vol. 9, 1952, pp. 381-389.

Several design specifications have been proposed and used for determining net area in tension members with staggered rows of holes. For one row of holes normal to the length of the member, subtracting the hole diameters from the gross width of the member is a rational rule for determining net width under the assumption of uniform stress across the section after plastic flow has occurred. For holes that are staggered across the normal section, the implications of an assumption of a uniformity of stress due to plastic deformation are not so obvious. Consider two staggered holes as in Fig. 1. There are two extreme possibilities: one, to take the net area across each normal section, i.e. $W-d$, as net width, and the other, to take out both holes, i.e. $W-2d$. Here, W is the gross width of the piece, and d the diameter of each hole. Intuitively, it would seem that the first case would be unsafe, and the second too conservative. The correct net width probably lies between these extremes, and, moreover, it seems likely that the correct net width is a function of the stagger and gage, stagger being defined as the spacing longitudinally between the centers of adjacent holes, and gage the transverse spacing between centers of two adjacent holes.

Many suggestions were advanced for design rules^{3,4} and in 1915 T. A. Smith⁵, on the basis of Cochrane's earlier work, published the following formula:

$$x = \frac{g}{d} - \frac{2(g^2 + s^2 - d\sqrt{g^2 + s^2})}{d(g + \sqrt{g^2 + 4s^2})} \quad (1)$$

where

x = the fractional part of a hole to be deducted,
 g = the distance between gage lines,
 s = the pitch or stagger, and
 d = the diameter of the hole.

Other formulas have been suggested as approximations to the Smith-Cochrane formula. One due to C. R. Young⁶ is

$$x = 1.50 - 1.25 s/g \quad (2)$$

Cochrane proposed⁷ the formula

3. "Some Tests Bearing on the Design of Tension Members", by Edward Godfrey, Engineering News, vol. 55, 1906, pp. 488-489.
4. "Calculating Net Section of Riveted Tension Members, and Fixing Rivet Stagger", by Victor H. Cochrane, Engineering News, vol. 59, 1908, p. 465.
5. "Diagram for Net Section of Riveted Tension Members", Engineering News, vol. 73, 1915, p. 893.
6. "True Net Sections of Riveted Tension Members", by C. R. Young, Engineering Research Bulletin No. 2, University of Toronto, 1921, pp. 233-244.
7. "Rules for Rivet-Hole Deductions in Tension Members", by Victor H. Cochrane, Engineering News-Record, vol. 89, 1922, pp. 847-848.

$$r = d - s^2 / 4g, \quad (3)$$

where r is the width of strip to be deducted. This is the formula in general current use, specified for calculating net area for sections with staggered holes by the AREA, the AISC, and the AASHO. The following quote is typical:

"The net width for any chain of holes extending progressively across the part shall be obtained by deducting from the gross width the sum of the diameters of all the holes in the chain and adding, for each gage space in the chain, the quantity:

$$s^2 / 4g$$

where s equals the pitch of any two successive holes in the chain, g equals the gage of the same holes.

The net section of the part is obtained from the chain which gives the least net width".

Tests to failure of drilled steel plates with two and three staggered holes were performed by C. R. Young and W. B. Dunbar⁸ who concluded that the Smith-Cochrane formula was somewhat too severe.

Clarence Holleman⁹ reports tests to failure on several aluminum alloys, as well as on SAE X4130 steel. Holleman recommends the use of a tension efficiency of 90% based on net area for tension members with holes when using aluminum alloys. C. H. Stevenson¹⁰ reports tests to failure on sheet specimens of several aluminum alloys with one and two holes drilled in various configurations. Stevenson reports increasing efficiencies as stagger is increased, but there are wide variations of efficiency of as much as 13% between the alloys tested. In the above papers, efficiency of a tension member is defined as the ratio of ultimate strength based on net area to the ultimate strength of a solid tensile specimen, expressed in per cent.

8. "Net Section of Drilled Plates", by C. R. Young and W. B. Dunbar, Engineering Research Pulletin No. 6, University of Toronto, 1926, pp. 51-65.
9. "Tension Joints in Aircraft Structures", by Clarence H. Holleman, Journal of the Aeronautical Sciences, vol. 10, 1943, pp. 295-302, 310.
10. "The Effects of Open Holes on the Tensile Strength of some Aluminum Alloys", by C. H. Stevenson, Symposium on Notch Effects in High-Strength Aluminum Alloys in the Journal of the Aeronautical Sciences, vol. 13, 1946, pp. 395-397.

H. N. Hill and R. S. Barker^{11,12} report tests on specimens cut from aluminum and magnesium alloy sheet, the tests being carried to failure. The specimens were taken at right angles to the direction of rolling. They reported that the specimens containing two staggered holes showed a reduced efficiency, based upon the $s^2/4g$ rule, the reduction increasing with increasing ratio of pitch to gage up to a ratio of 1. They also reported that the greatest reduction in ultimate strength was found for the most ductile materials.

Unfortunately, as none of these papers reported limit load data, no direct comparison can be made with the present tests.

The hole patterns discussed in this paper were chosen so as to give the same least net area for two or more rows of holes as for one row using the $s^2/4g$ rule; see Fig. 2. The configurations were the one row case (1), the two row case (1, 2U), the three row cases (1, 2U, 3U) (2L, 1, 2U) termed 3S and 3L respectively, the five row case (3L, 2L, 1, 2U, 3U), and all nine rows. Thus, on the basis of the $s^2/4g$ criterion, the sheets with one or more rows should all have the same limit load.

Limit Analysis Theorems

The limit theorems offer a method of determining upper and lower bounds for the limit load of any perfectly plastic material and therefore avoid the almost impossible exact plastic analyses which would otherwise be required. This method will be described as applied to perfectly plastic materials, in a state of plane stress, which obey the maximum shearing stress criterion of Tresca. According to this criterion, plastic deformation occurs only when the maximum shearing stress has reached a value k , the yield stress in pure shear. Perfect plasticity implies that the maximum shearing stress cannot exceed k . If principal stresses σ_1, σ_2 are employed as Cartesian coordinates ($\sigma_3 = 0$), the states of stress with the maximum shearing stress k are represented by the points of the hexagon ABCDEF in Fig. 3.

The principal axes of the plastic strain rate or increment in an isotropic material coincide with the principal axes of stress. The principal plastic strain rates are denoted by $\dot{\epsilon}_1, \dot{\epsilon}_2$, and $\dot{\epsilon}_3$, and are in the directions of σ_1, σ_2 , and σ_3 respectively. If the plastic strain rate is represented by a vector with principal components $\dot{\epsilon}_1, \dot{\epsilon}_2$, and if strain axes are superposed on the stress axes, this "vector" is outwardly normal to the hexagon representing the state of stress in plastic flow¹³ as shown in Fig. 3. At the

11. "Effect of Open Circular Holes on Tensile Strength and Elongation of Sheet Specimens of some Aluminum Alloys", by H. N. Hill and R. S. Barker, NACA Technical Note 1974, 1949.
12. "Effect of Open Circular Holes on Tensile Strength and Elongation of Sheet Specimens of a Magnesium Alloy", by R. S. Barker, NACA Technical Note 2716, 1952.
13. "Some Implications of Work-Hardening and Ideal Plasticity", by D. C. Drucker, Quarterly of Applied Mathematics, vol. 7, 1950, pp. 411-418.
 "A More Fundamental Approach to Stress-Strain Relations" by D. C. Drucker, Proceedings First U. S. National Congress of Applied Mechanics, June 1951, pp. 487-491.

vertices, the direction of the vector representing the plastic strain rate may lie anywhere between, and including, the directions of the plastic strain rate determined by the two adjacent sides of the hexagon. It should be noted that the incompressibility condition $\dot{\epsilon}_1 + \dot{\epsilon}_2 + \dot{\epsilon}_3 = 0$ determines $\dot{\epsilon}_3$ when $\dot{\epsilon}_1$ and $\dot{\epsilon}_2$ are known.

When a tension member with a row of holes is loaded, the strains are purely elastic at first. As the loading is continued, the maximum shearing stress at points on the boundary of the holes becomes equal to k in magnitude and plastic flow may take place. Further increase in load causes the plastic regions to grow but they are initially completely contained in regions in which the strains are still elastic. The strains in the plastic regions, therefore, will still be of the same order of magnitude as the elastic strains in the surrounding regions. This state, after Prager, is called contained plastic flow. At some load, often after regions of plastic flow have reached completely across the member, the plastic region is no longer constrained by elastic regions. The load at which this occurs is called the limit load, and the member is now in a state of impending plastic flow. In the cases considered here, large plastic deformations will then take place at no increase in load.

The first basic limit analysis theorem* states that the limit load is the largest load for which a statically admissible stress field may be found. A statically admissible stress field is here defined as one which

- (a) satisfies equilibrium everywhere,
- (b) satisfies the stress boundary conditions, and
- (c) has nowhere a maximum shearing stress larger in magnitude than k .

Such a stress field may be discontinuous as will be seen later.

The second basic theorem states that the limit load is the lowest load for which a kinematically admissible velocity field can be found. A kinematically admissible velocity field is here defined as one in which strain rates are to be considered as plastic only and

- (a) the incompressibility condition is satisfied, and
- (b) the rate at which work is done by the external loads or surface tractions is equal to, or exceeds, the internal rate of dissipation of energy for the whole body under consideration.

This theorem remains valid for velocity fields with surfaces of discontinuity through which the velocity component normal to the surfaces varies continuously while the tangential component is discontinuous. These surfaces may be treated as the limiting cases of a transition layer with continuous but rapidly varying, tangential velocity components.

For plane stress and continuous velocity distributions, the internal rate of dissipation of energy per unit volume is expressed by

$$D = c_1 \dot{\epsilon}_1 + c_2 \dot{\epsilon}_2 \quad (4)$$

The internal rate of dissipation of energy for the entire body is obtained by integrating the expression (4) over the volume of the body. Note that the internal rate of dissipation of energy for plane stress fields is the scalar

*For proofs of these theorems, see references 1 and 2.

product of the vector from the origin to one of the stress points on the hexagon of Fig. 3, and the vector representing the plastic strain rate. It may be written as

$$D = 2k \max |\dot{\epsilon}| \quad (5)$$

where $\max |\dot{\epsilon}|$ is the magnitude of the absolutely largest principal component of the plastic strain rate $\dot{\epsilon}_1$, $\dot{\epsilon}_2$, or $\dot{\epsilon}_3$ ^{14,15}. For a surface of discontinuity, the rate of internal energy dissipation per unit area at any point in the surface is

$$D_A = kv \quad (6)$$

where v is the change in the tangential velocity component across the surface of discontinuity at the point. The total rate of internal energy dissipation for the whole surface is obtained by integrating (6) over the area of the surface.

The rate at which work is done by the external loads or surface tractions may be computed once a velocity field has been determined.

Limit Loads for Patterns of Circular Holes

Consider now the computation of upper and lower bounds of the limit loads for each of the six configurations tested:

(a) One row configuration of five holes. A stress field consisting of uniaxial tension in strips lying longitudinally between the holes is statically admissible if the tensile stress does not exceed $2k$, Fig. 4a. Note that the end boundary conditions on the sheet are simply that the sheet is pulled by rigid bars rather than that uniform stress is applied. As the sheet widens out at the end, however, the two cases are in fact equivalent. Then

$$T^* \geq t(W - 5d) 2k, \quad (7)$$

where

- T^* = the limit load for the sheet,
- t = the thickness of the sheet,
- W = the width of the sheet,
- d = the diameter of the holes,

and

$2k$ = the stress in the strips between the holes.

14. "Limit Design of Reinforcements of Cut-Outs in Slabs", by P. G. Hodge, Jr. and W. Prager, Brown University Report B11-2 to the Office of Naval Research, 1951.
15. "The Application of Limit Analysis to Punch Indentation Problems" by R. T. Shield and D. C. Drucker, to appear in Journal of Applied Mechanics.

$$T_0 = 2kwt, \quad (8)$$

a lower bound for the ratio T^*/T_0 , is

$$T^*/T_0 = (W - 5d)/W. \quad (9)$$

One kinematically admissible velocity field for the one row configuration is shown in Fig. 4b, half of the sheet sliding with velocity v along a section through the holes 45° out of the plane of the sheet. Here,

$$D_A = kv \quad (10)$$

for the whole discontinuity surface, and the total rate of internal energy dissipation is kv times the area of the surface. Thus, for very thin sheets, the total internal energy dissipation rate is

$$E_i = \sqrt{2} t(W - 5d) kv, \quad (11)$$

The rate of external work done on the sheet by the tensile load T is

$$E_e = Tv / \sqrt{2} \quad (12)$$

Equating (11) and (12) gives T which is here an upper bound for the limit load T^* so that

$$T^*/T_0 \leq (W - 5d)/W. \quad (13)$$

The same result is obtained with the symmetric discontinuous velocity pattern of Fig. 4c. As the upper and lower bounds coincide, the solution for the limit load is exact for the maximum shearing stress criterion within the assumptions of the theory for very thin sheets, and

$$T^*/T_0 = (W - 5d)/W = 0.75 \quad (14)$$

for $W = 10$ inches and $d = 1/2$ inch.

The restriction to sheets of thickness small compared to the diameter of hole is clear from Fig. 4. Out of plane sliding on a 45° angle would take place on an appreciably larger area than $(W - 5d) t\sqrt{2}$ for thick plates.

(b) Nine row configuration. A statically admissible stress field which takes out all the holes similar to that for the one row configuration gives

$$T^* \geq (W - 9d)2k, \quad (15)$$

and

$$T^*/T_0 \geq (W - 9d)/W = 0.55. \quad (16)$$

A simple kinematically admissible velocity field is obtained by letting one portion of the sheet slide on two sets of planes perpendicular to the plane of

the sheet and through the nine holes on a 45° plane as shown in Fig. 5a. Here again, the internal dissipation, E_1 , is k times the area of the surface of sliding multiplied by the discontinuity velocity v , or

$$E_1 = [W\sqrt{2} - (8d + \sqrt{2}d)]t kv \quad (17)$$

The rate at which work is done by the external force is

$$E_0 = Tv/\sqrt{2} \quad (18)$$

Equation (17) and (21) gives

$$T^*/T_0 \leq kt[2W - (8\sqrt{2} + 2)d] \quad (19)$$

or

$$T^*/T_0 \leq 1 - (4\sqrt{2} + 1) \frac{d}{W} = 0.67 \quad (20)$$

This result may be improved by changing the angle of sliding slightly, Fig. 5b. Although $L' + 4L$ is increased, $v \cos \alpha$ likewise gets larger. An angle $\beta = 28^\circ$, corresponding to $\alpha = 36^\circ$ results in

$$T^*/T_0 \leq 0.63 \quad (21)$$

(c) Two row configuration. The stress field which was used for the nine row configuration is statically admissible for the two row configuration. Also the velocity field used for the one row configuration is a kinematically admissible velocity field for the two row configuration. Thus

$$0.55 \leq T^*/T_0 \leq 0.75 \quad (22)$$

In fact, these are bounds for all configurations with two or more rows of holes.

To improve the lower bound, consider the stress field which is a superposition of the stress fields shown in Fig. 6a and 6b. The shaded regions are isotropic stress regions, $\sigma_1 = \sigma_2$. A detail of the manner in which the stress field is taken through the holes is shown in Fig. 7. Fig. 6b incorporates a discontinuous stress field¹⁵ the details of which are sketched in Fig. 8a. The maximum shearing stress is not increased when the stress field of Fig. 6b is superposed on the stress field of Fig. 6a if the angle $\theta = 35^\circ$ and c is made as large as possible as shown in Fig. 8a. For the present configuration, for $\gamma = 19.9^\circ$, which minimizes L'' , and for $\theta = 35^\circ$, a lower bound on T^*/T_0 is 0.70. Therefore, for the two row configuration,

$$0.70 \leq T^*/T_0 \leq 0.75. \quad (23)$$

(d) Three row configuration 3-S (1, 2U, 3U). Here also a similar stress field to that applied to the two row configuration may be used, Fig. 8b. The geometry is such that an angle $\theta = 33^\circ$ for the discontinuous portion of the stress field is possible without increasing the maximum shear. However, the excess side tensile force is twice as large as for the two row configuration,

hence the lower bound of the limit load is correspondingly reduced. For the present configuration,

$$T^*/T_0 \geq 0.66 \quad (24)$$

A kinematically admissible discontinuous velocity field is shown in Fig. 9a, the upper portion of the sheet moving up with velocity v , the lower portion moving down with velocity v , and the two wedges, ABC and DEF, moving laterally with velocity $v' = v \tan \alpha$. The details of the velocity field along BD are shown in Fig. 9b. The upper bound on T^*/T for the simplest case of $\alpha = 45^\circ$ is 0.73 and for $\alpha = 36^\circ$ is 0.72, therefore,

$$0.66 \leq T^*/T_0 \leq 0.72 \quad (25)$$

(e) Three row configuration 3-L (2L, 1, 2U). Fig. 8c shows a statically admissible field somewhat more elaborate than for the two row case which gives

$$T^*/T_0 \geq 0.67 \quad (26)$$

(f) Five row configuration. A velocity field of the type applied to the (1, 2U, 3U) 3-S three row configuration is used here, as shown in Fig. 10. The upper bound for $\alpha = 45^\circ$ is 0.71 and for $\alpha = 36^\circ$ is $T^*/T_0 = 0.69$. A stress field more elaborate still than in Fig. 8 determines a lower bound of 0.58 so that

$$0.58 \leq T^*/T_0 \leq 0.69. \quad (27)$$

The lower bound is not much of an improvement over the 0.55 of Eq. (16).

Limit Loads for Patterns of Square Holes

It is of some interest to note that if the holes in the one row and nine row configurations were half inch squares, the limit loads would be exactly

$$T^*/T_0 = 0.75 \quad (28)$$

for the one row configuration, and

$$T^*/T_0 = 0.55 \quad (29)$$

for the nine row configuration. Fig. 11 shows the symmetric 45° velocity pattern which gives the same result as the simple one-plane slide of the type shown in Fig. 5.

The $s^2/4g$ Rule

A load carrying plate in a riveted joint which is transmitting some or all of its load to cover plates or other members differs essentially from the perforated plates just described. The rivets do not act simply as plugs but take load out of the plate, Fig. 12. Yielding in the sense of reaching a limit load may occur across the first rivet holes or by some combination of first and second holes, but generally will not involve additional rows because the

loaded rivets interfere. One possible pattern is yielding in zones extending between the holes as shown in Fig. 13. The lower portion of the plate is assumed to move in the direction of T with a velocity v . Each zone inclined at α to the direction of T is then stretched at a speed $v \sin \alpha$ and sheared at $v \cos \alpha$. For a very thin plate, using the maximum shearing stress criterion, this is equivalent to stretching at a speed

$$v' = \frac{v \sin \alpha}{2} + \sqrt{\left(\frac{v \sin \alpha}{2}\right)^2 + \left(\frac{v \cos \alpha}{2}\right)^2} = \frac{v}{2} (\sin \alpha + 1) \quad (30)$$

in analogy to $\epsilon_{\max} = \frac{\epsilon}{2} + \sqrt{\left(\frac{\epsilon}{2}\right)^2 + \left(\frac{\gamma}{2}\right)^2}$ the expression for maximum strain in terms of the normal strain ϵ and shearing strain γ . An upper bound on the contribution to T_1^* from the length L of the zone of yielding is then obtained from

$$T_1^* v \leq T_1 v = 2kv'Lt$$

where t is the thickness of the plate. Thus

$$T_1^* \leq ktL (1 + \sin \alpha) \quad (31)$$

If, as shown in Fig. 13, the zone of yielding is taken to extend between the horizontal diameter extremes at the holes so that

$$L \sin \alpha = b, \quad L^2 = b^2 + s^2 \quad (32)$$

then

$$\begin{aligned} T_1^* &\leq kt (\sqrt{b^2 + s^2} + b) \\ &= ktb (\sqrt{1 + s^2/b^2} + 1) \\ &= ktb (2 + s^2/2b^2 - \dots) \\ &= 2ktb (1 + s^2/4b^2 - \dots) \end{aligned} \quad (33)$$

which is in a sense an $s^2/4b$ rule for the range of s small compared with b and is close to the $s^2/4g$ specification. This upper bound can be improved a little (i.e. lowered) by choosing a better value of α . It appears that $s^2/4g$ is a reasonable answer for riveted joints where the rivets take load out of the plate considered.

Mises Criterion of Yielding

If the Mises criterion is employed instead of the maximum shearing stress criterion as discussed so far, the yield curve is the circumscribing ellipse to the hexagon of Fig. 3. The shearing stress on the planes of sliding discontinuity is then larger in the ratio $2/\sqrt{3}$ or 1.155. All computed upper bounds for the perforated plates are therefore increased by a little more than 15%. Lower bounds remain lower bounds and considerably more elaborate stress patterns would be needed to raise them.

Experimental Program

Low carbon, hot-rolled steel sheet was used in the first series of tests because of its flat yield, and because it was hoped that the mechanical properties would be uniform enough so that the tests would not be complicated by local variations of these properties. The variation in yield strength was so large that several additional series of tests were run on hot-rolled steel sheet.

A 61S-T6 aluminum alloy was chosen to check the results with a material which has a much smaller ultimate elongation than hot-rolled steel, and which does not have a truly flat yield, Fig. 14.

All specimens were cut with the long dimension in the direction of rolling from sheet approximately 1/16 inch thick.

The sheet thickness was measured to ± 0.0002 of an inch at the intersection points of a one inch grid ruled over the central 10 inch long test section of each sheet. The readings for each sheet were averaged, the average being taken as the sheet thickness. The sheet widths were machined to 10.000 ± 0.005 inches, and the 0.500 inch diameter holes were drilled by means of a carefully laid out jig. Lubricated spherical seats and nuts were incorporated in the grip system. Two extensometers, designed for simplicity and ruggedness, were mounted one on each edge of the sheet with a 10 inch gage length. As a check on the performance of the grips, a dial gage was used to measure the relative displacement of the heads of the testing machine. The testing machine used showed a maximum error of plus 0% and minus 0.3%, in a recent calibration. The general test set-up is shown in Fig. 15.

The test pieces were pulled to a total extension, in the 10 inch gage length, sufficiently large to ensure flow across the specimen, and were not purposely carried to fracture.

Originally, it had been hoped that uniformity of mechanical properties would allow the accurate determination of the yield stress of the material in each series from three test pieces with no holes. However, uniformity was the exception and it was necessary to cut tension test coupons from the test pieces themselves, or to use pieces at each end of each large test piece, for the purpose of determining the yield stress of that particular test piece. Coupons 9.5 inches wide could be obtained from the test specimens because yielding in the 10 inch specimens was confined to the region of the holes. In the calculations, the yield stress for each large test piece was taken arbitrarily to be the average obtained from the test coupons from that piece. This point will be discussed in more detail later.

Photographs of the flaked scale patterns of representative hot-rolled steel test pieces are shown in Fig. 16. It should be noted that these photographs show the pattern after the tests were completed. However, the patterns are interesting in that the tendency to yield along the diagonal through the holes is clearly shown for configurations with two or more rows of holes. Visual observation of the one row configuration during tests established that the yield occurred initially along a transverse section through the holes, as assumed for the velocity field in the analysis. One sheet was tested with strain gages mounted in the transverse section through the holes to establish the limit load very accurately and to demonstrate that large strains occur for a small bend in the overall load deformation curve.

A series of curves for specimens from one large sheet of hot-rolled steel is shown in Fig. 17. The ordinate is made dimensionless by dividing the limit load by the product of the "average" yield stress and the gross area.

Starting with the one row configuration, the limit load is marked by hardly more than an indentation in the curve; the curves then flatten out increasingly at the limit load as the number of rows of holes is increased. For the nine row configuration, there are marked upper and lower yields. Fig. 18 is a similar set for the 61S-T6 specimens which exhibit the same general pattern except, of course, for the absence of an upper yield. Placing plugs in the holes has small effect in any case, except for details of shape.

Figs. 19a and b demonstrate the very large scatter which was obtained for the hot-rolled steel sheets. To avoid confusion, the 1, 3, and 9 row cases are separated from the 2 and 5 row. All curves are brought in tangent to the average elastic line by slight displacements left or right to minimize distortion of shape. Each limit load selected is indicated by a small arrowhead, because in several cases the choice was quite arbitrary. The symbol P indicates that the holes were fitted with plugs of almost no clearance. Despite the scatter, the conclusion is unmistakably that there is an appreciable and significant difference between the limit loads for the different configurations of holes.

The questions which should be answered are why the data for any one configuration of holes covers so wide a range and which of the values should agree with the theory of limit analysis. The temptation is to take the average value and, if this is done, agreement is obtained in principle with the limit analysis theory although values are above those calculated with the maximum shearing stress criterion. An average for the purpose of comparison of theory and experiment is proper, however, if the deviations are due to haphazard factors only, such as experimental error. There would seem to be no possibility in these tests of instrumental error of appreciable magnitude compared with the observed variations so that averaging is suspect.

Some oversimplified examples explain the difficulty and indicate that the lower values of T^*/T_0 , the stress ratio, are the ones which should agree with an idealized theory. Suppose first that the yield stress is constant across the sheet but varies periodically between 25000 and 30000 along the length of the sheet. If there are no holes, a yield stress of 25000 will be found experimentally because the weakest section will govern. A sheet with one row of transverse holes will exhibit a variation in limit load corresponding to the range of 25000 to 30000, or over 15 per cent, depending upon whether the line of holes is located in a weak or a strong region. If a large number of tests are run, the results will scatter as in Fig. 19 and clearly the answer which should agree with theory is the lowest limit load obtained, barring experimental error. On the other hand, if the yield stress varies in the transverse direction but is constant along the length of the sheet, a specimen without holes will test at the average value of 27500 and the average of the one row cases should be compared with theory. In general, the variation in yield stress will not follow either pattern and will tend to be somewhat random in addition. Under these conditions in most cases there will be some way for the large test coupons, without holes, to yield at a value close to 25000 while the sheets with holes will usually have stronger regions impeding plastic deformation. The lower values of limit load, although not necessarily the lowest, should then correspond to the theory.

A variation in thickness has an analogous effect to a variation in yield stress but in the experiments did not exceed 2% while the yield stress determined by small test coupons in one extreme case varied by more than 25% over the entire sheet. An interesting verification of the importance of local variations in yield is provided by a comparison of yield stress obtained from

the small test coupons, approximately 3 square inches of sheet, and the large test coupons of 20 to 60 times this area of sheet. Several cases were obtained of small coupons ranging from 25000 to 29000 while the large coupons in the same region of the sheet tested between 25000 and 26000.

A summary of all experimentally determined stress ratios, T^*/T_0 is given in Fig. 20 whose points are subject to considerable latitude in their position. A glance at Figs. 17-19 shows that the limit load is not defined precisely in most experiments with a work hardening material. All indications are nevertheless that the answers of maximum shear stress theory are reasonable for an ideal homogeneous material. However, as usual, a compromise between the Mises and the maximum shear stress criteria will probably be better. The dimensionless plot enables comparison of the data for aluminum and steel. Results for aluminum are in the low range of the results for steel. As the aluminum is quite uniform in its properties, this seems to provide further confirmation of the influence of variable yield stress in the steel sheet.

Conclusion

Both the limit analysis and the tests show clearly that the configuration of holes is important in a sheet under tension and must be taken into account for an accurate analysis of open or plugged holes. As might be expected this is not done properly by the $s^2/4g$ rule for riveted joints. The specification rule is shown to be based conceptually on an upper bound computation for riveted joints in which the rivets take load out of the sheet being analyzed.

The value of 0.75 for T^*/T_0 is given by the rule for all configurations of holes tested. This is appreciably above many of the test results which range from 0.63 to 0.92 depending on the number of rows of holes and the uniformity of the test specimen.

Acknowledgment

The authors wish to express their appreciation to Robert Carlson and Anthony Gemma for carrying out many of the check tests, to William Johnson for machining all the specimens and to C. K. Liu and F. D. Stockton for helpful advice.

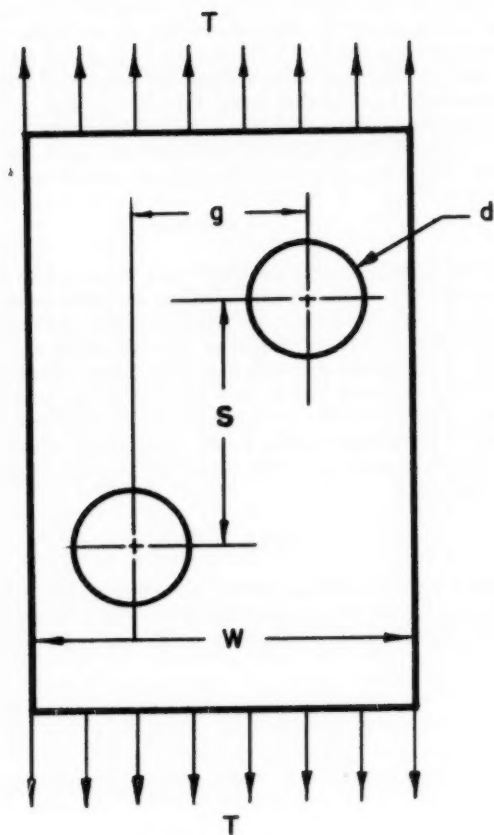


FIG. 1. TENSION MEMBER WITH TWO STAGGERED HOLES

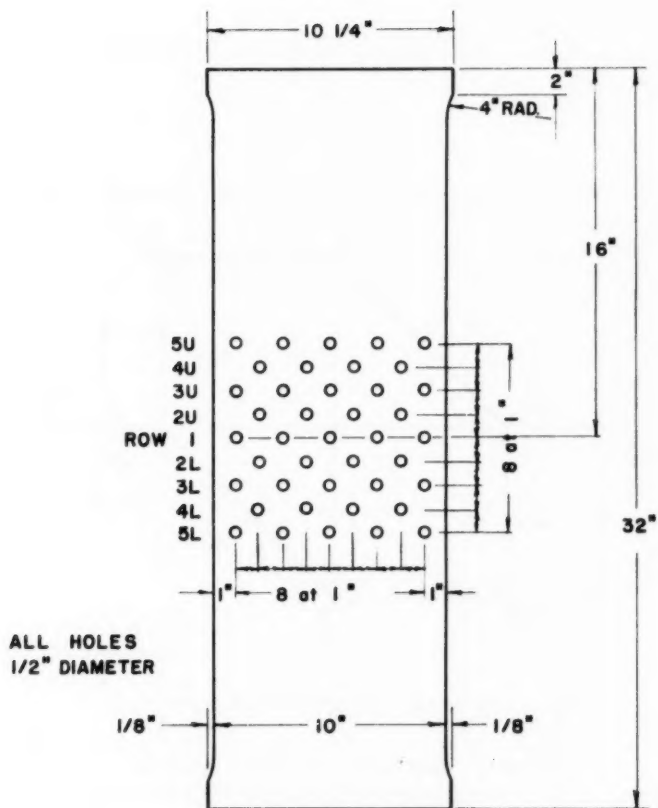


FIG. 2 TEST PIECE CONFIGURATION

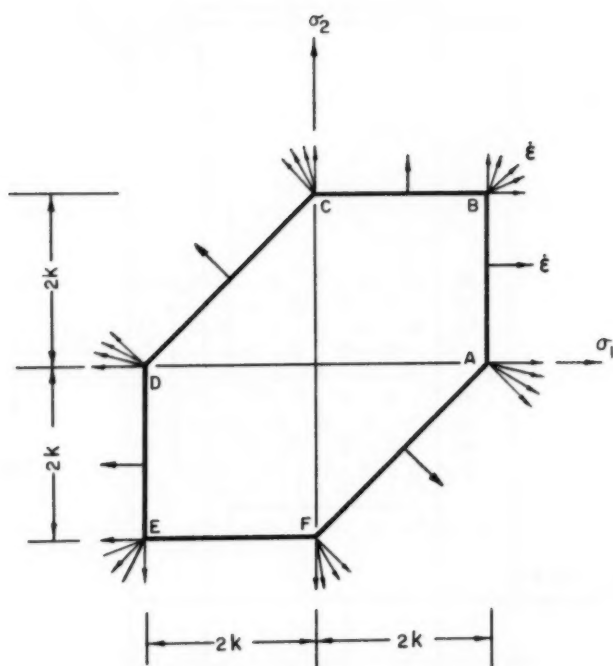


FIG. 3. MAXIMUM SHEARING STRESS
CRITERION FOR PLANE STRESS

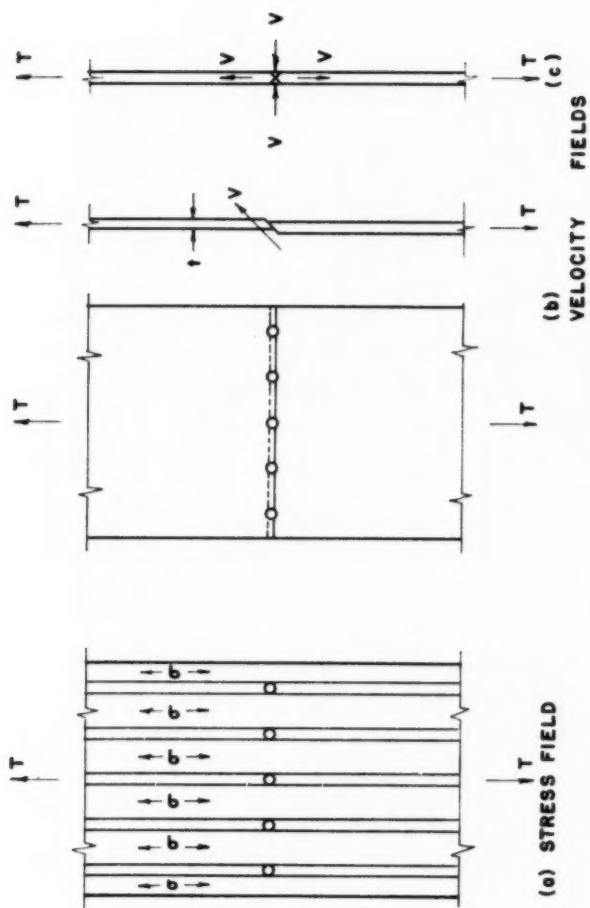


FIG. 4 ONE - ROW CONFIGURATION

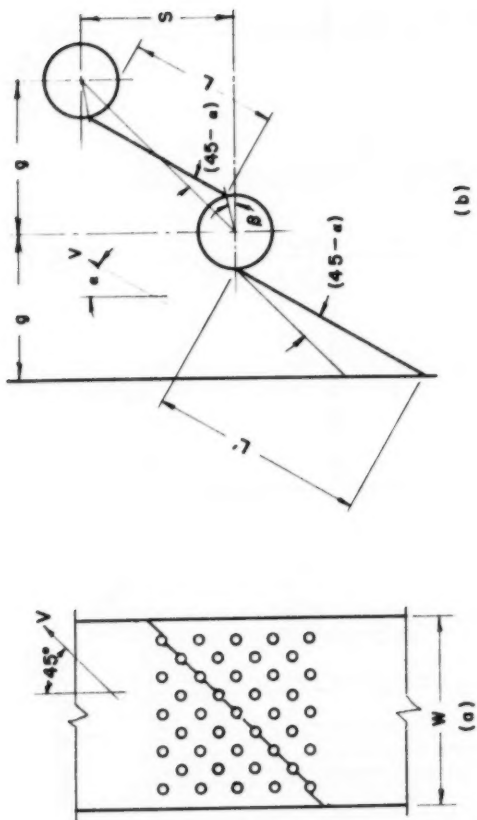


FIG. 5 VELOCITY FIELDS FOR NINE-ROW CONFIGURATION

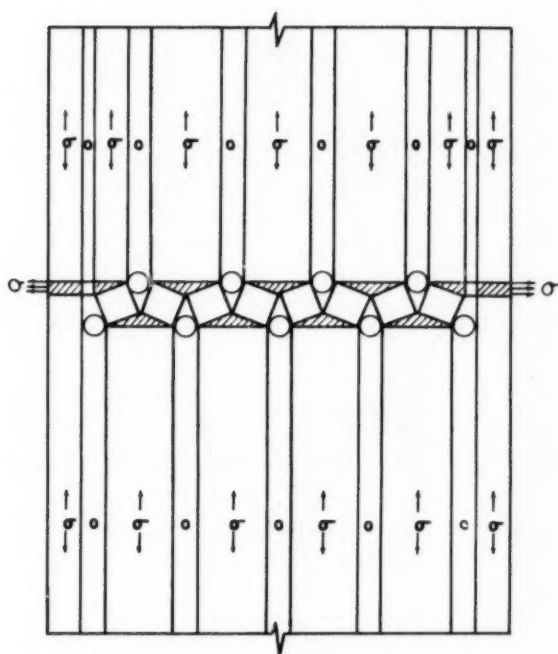


FIG. 6a. PART OF STRESS FIELD,
TWO ROW CONFIGURATION

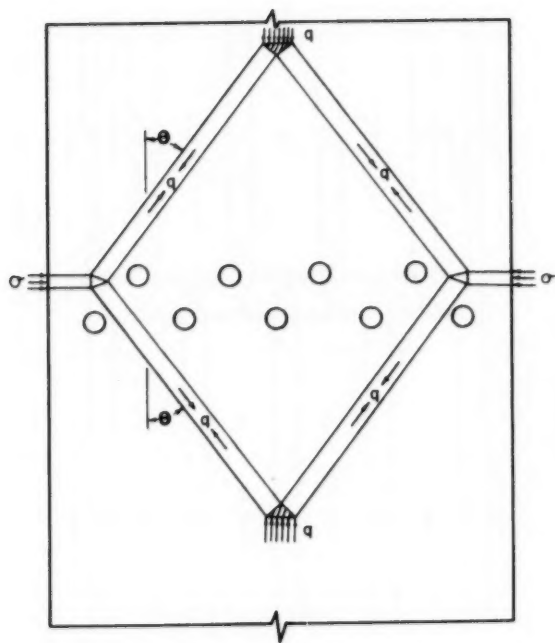


FIG. 6b. REMAINDER OF STRESS FIELD,
TWO ROW CONFIGURATION

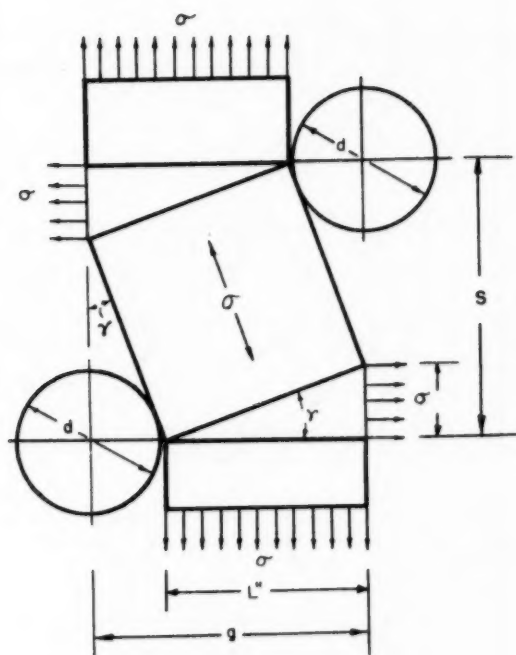


FIG. 7. DETAIL OF STRESS FIELD THROUGH HOLES

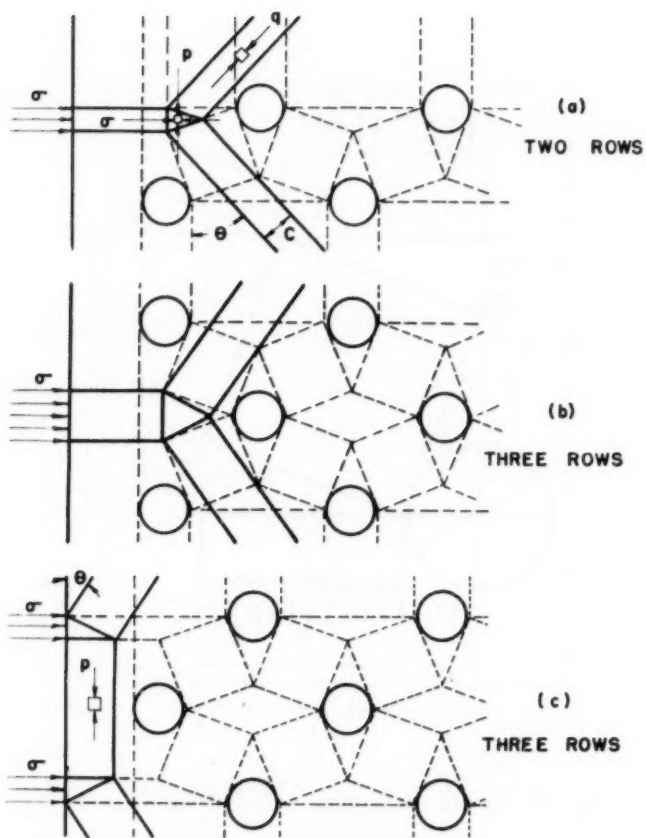
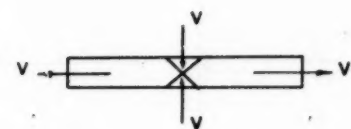
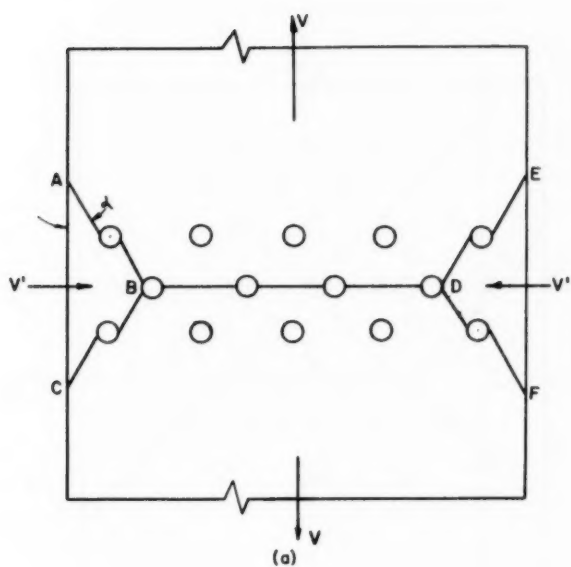


FIG. 8 DISCONTINUOUS STRESS FIELDS



(b) DETAIL, SECTION B-D

FIG. 9. VELOCITY FIELD, 3-L ROW CONFIGURATION

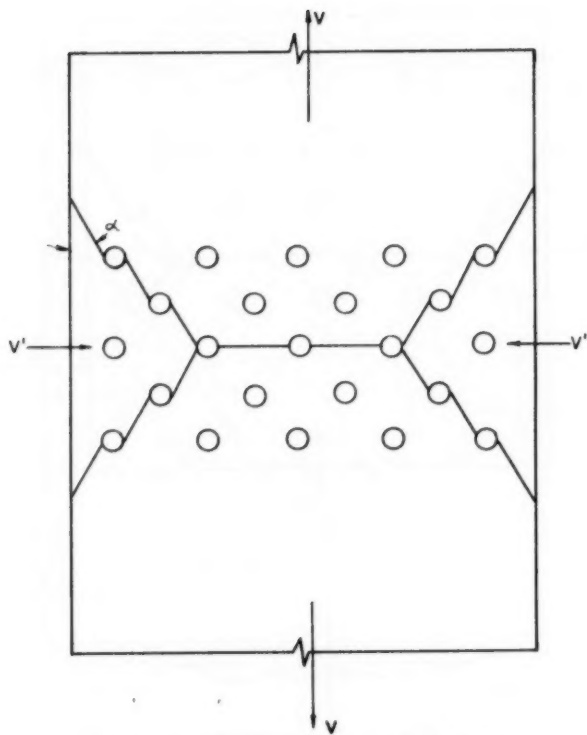
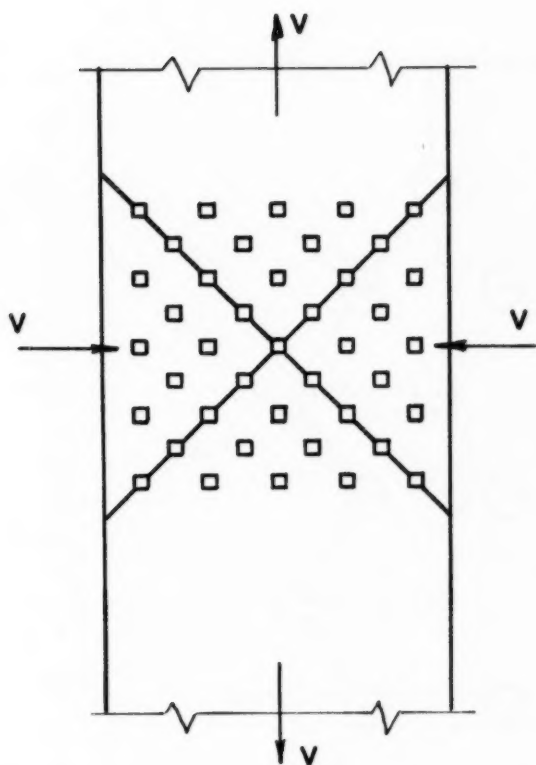
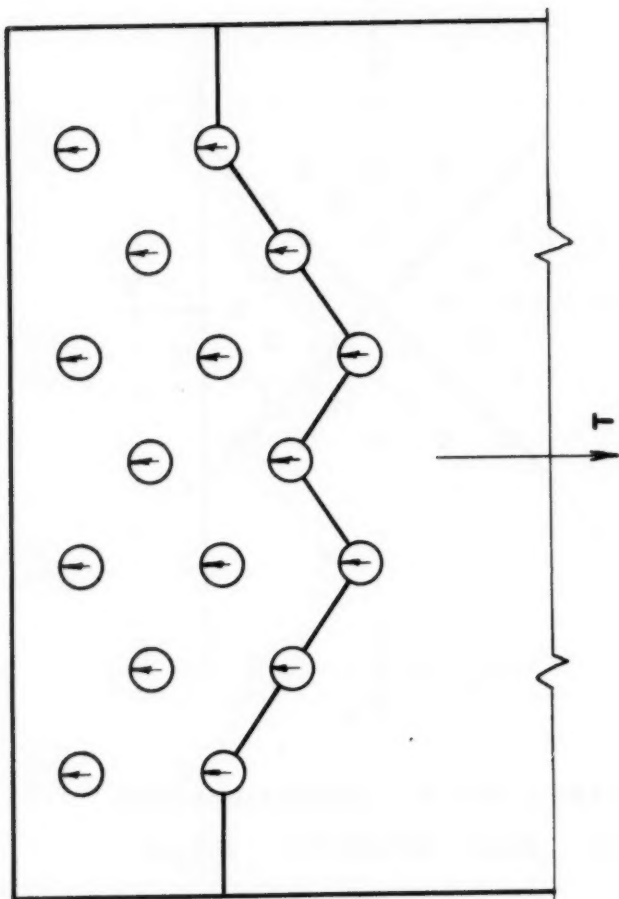


FIG. 10. VELOCITY FIELD, FIVE ROW
CONFIGURATION



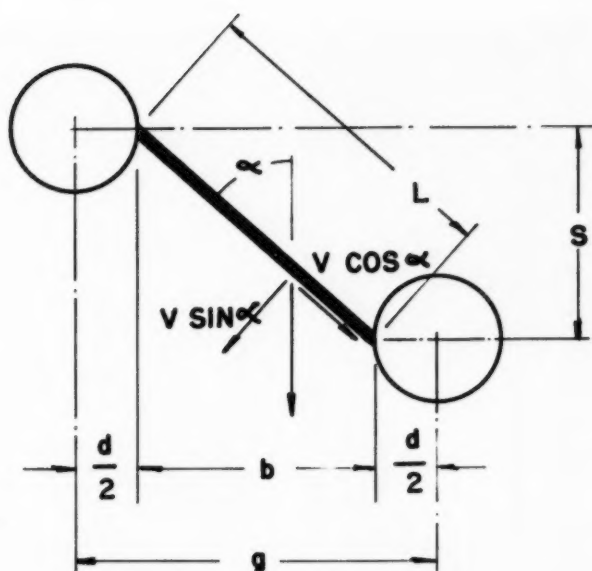
SQUARE HOLE CONFIGURATION
NINE ROW VELOCITY FIELD

FIG. II



RIVETED JOINT

FIG. 12



$S^2/4g$ RULE

FIG. 13

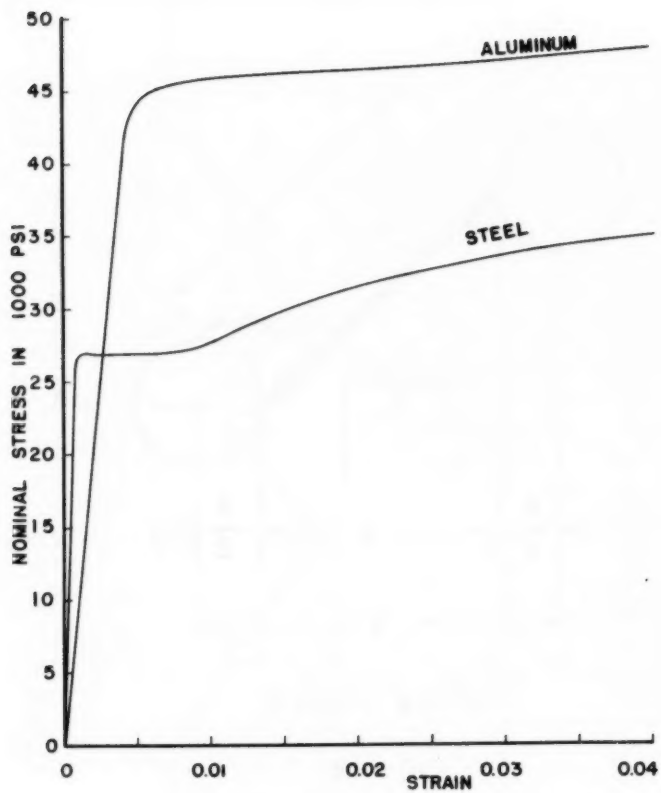


FIG.14 STRESS - STRAIN CURVES FOR STEEL AND ALUMINUM SHEET

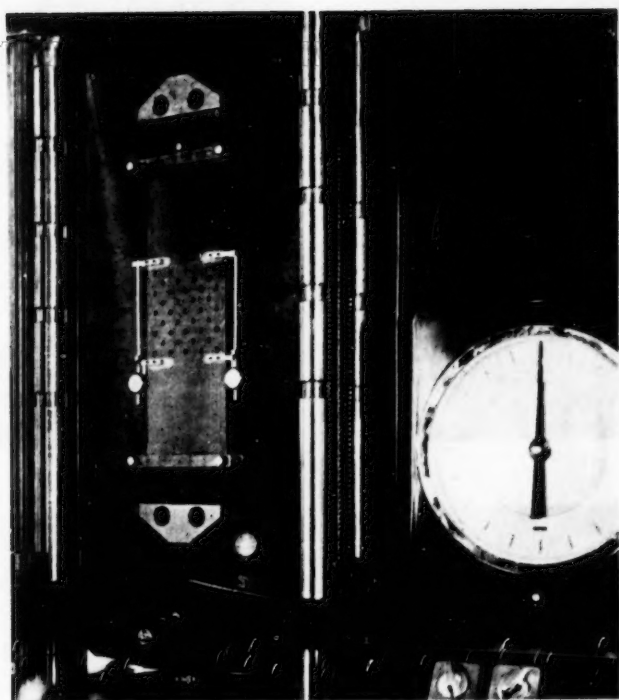


FIG. 15. TEST SET-UP

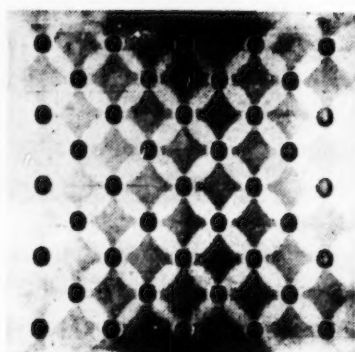
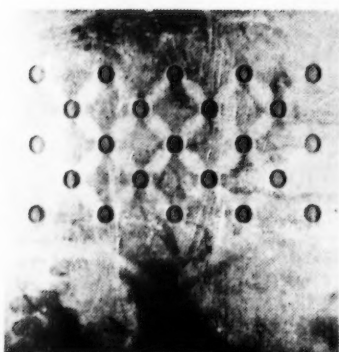
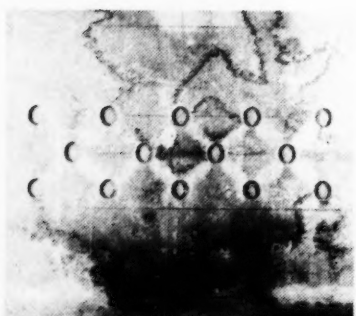
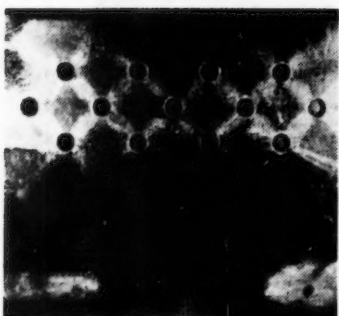
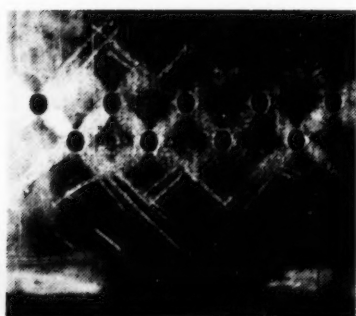
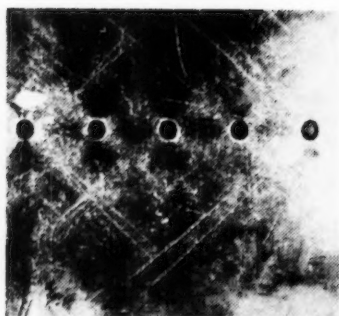


FIG. 16. YIELD PATTERNS

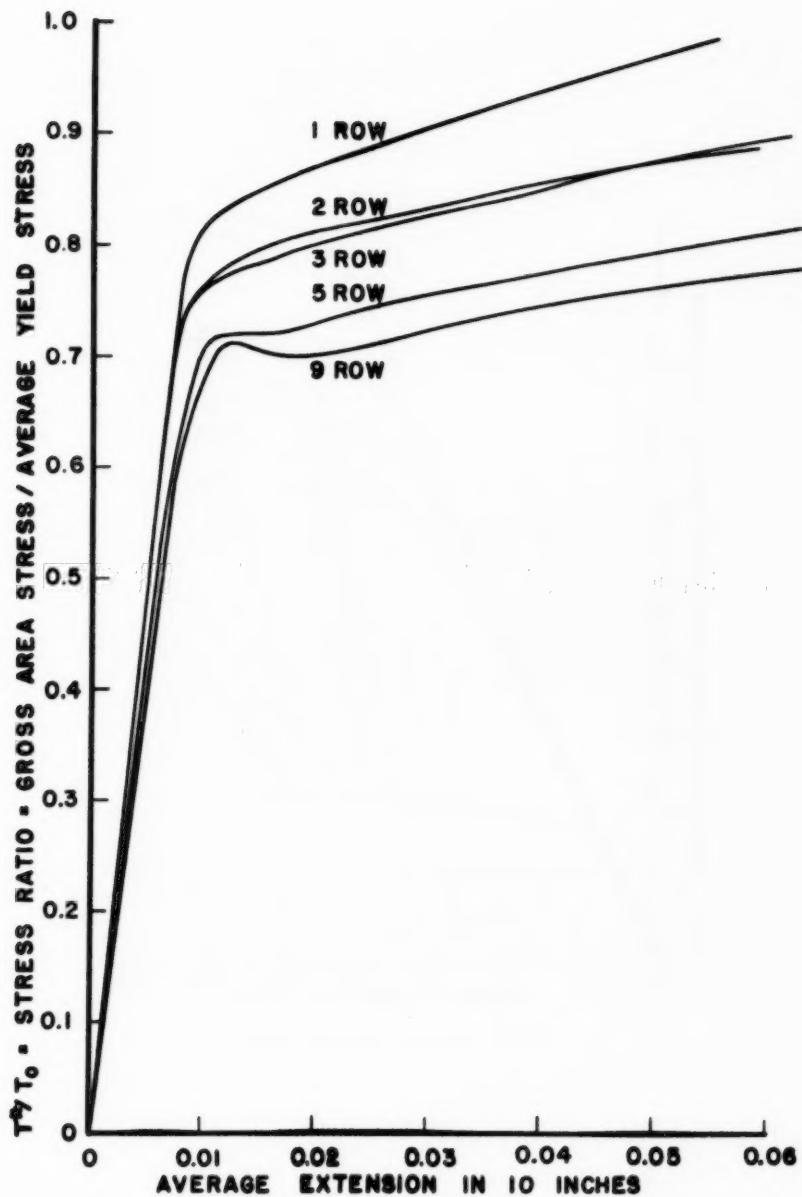


FIG. 17 TYPICAL HOT ROLLED STEEL SHEET RESULTS

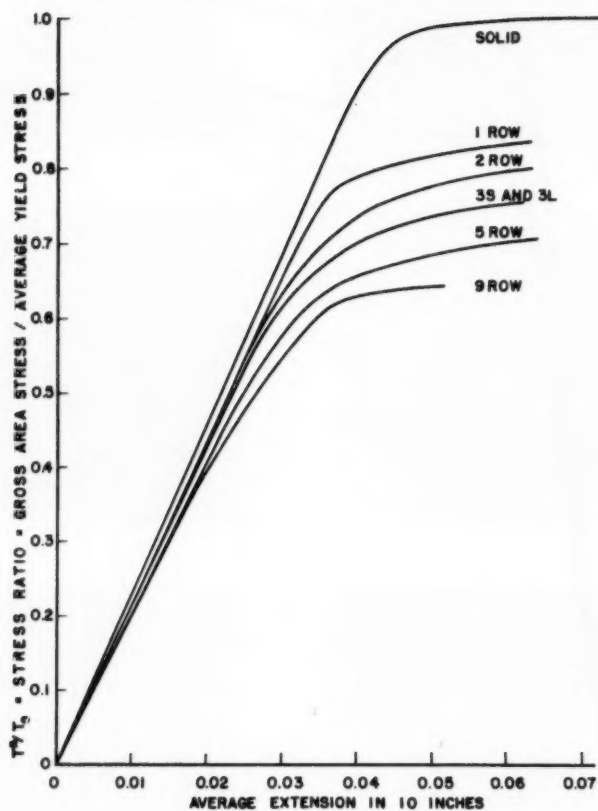


FIG. 18 61S-T6 ALUMINUM SHEET

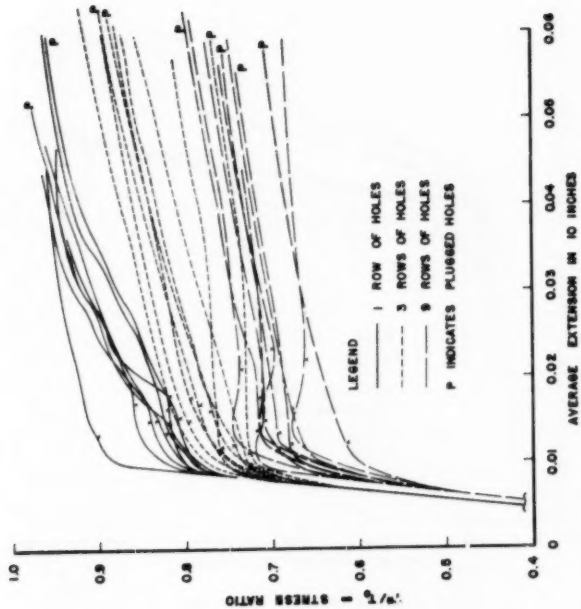


FIG. 19 A SCATTER OF TEST RESULTS

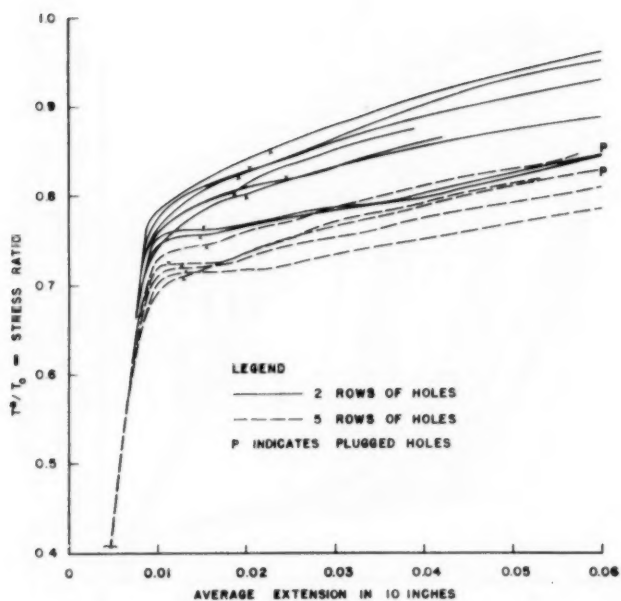


FIG. 19B SCATTER OF TEST RESULTS

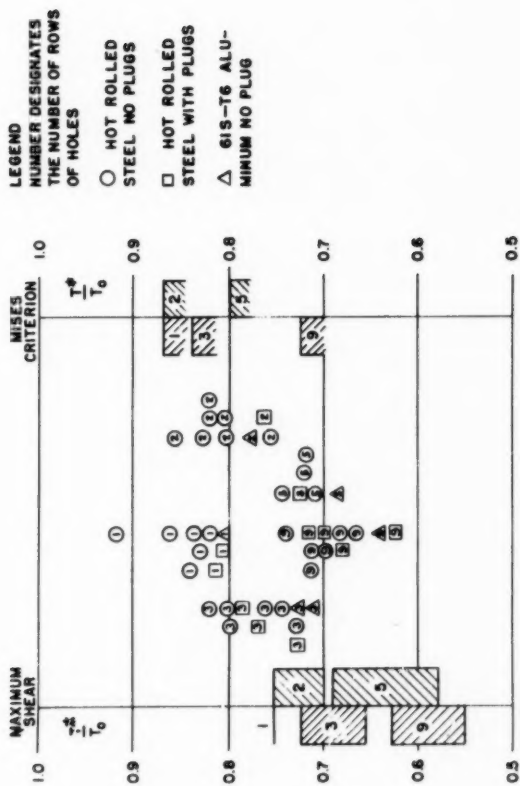


FIG. 20 SUMMARY OF TEST DATA

AMERICAN SOCIETY OF CIVIL ENGINEERS

OFFICERS FOR 1953

PRESIDENT

WALTER LEROY HUBER

VICE-PRESIDENTS

Term expires October, 1953:

GEORGE W. BURPEE
A. M. RAWN

Term expires October, 1954:

EDMUND FRIEDMAN
G. BROOKS EARNEST

DIRECTORS

Term expires October, 1953:

KIRBY SMITH
FRANCIS S. FRIEL
WALLACE L. CHADWICK
NORMAN R. MOORE
BURTON G. DWYRE
LOUIS R. HOWSON

Term expires October, 1954:

WALTER D. BINGER
FRANK A. MARSTON
GEORGE W. McALPIN
JAMES A. HIGGS
I. C. STEELE
WARREN W. PARKS

Term expires October, 1955:

CHARLES B. MOLINEAUX
MERCEL J. SHELTON
A. A. K. BOOTH
CARL G. PAULSEN
LLOYD D. KNAPP
GLENN W. HOLCOMB
FRANCIS M. DAWSON

PAST-PRESIDENTS

Members of the Board

GAIL A. HATHAWAY

CARLTON S. PROCTOR

TREASURER

CHARLES E. TROUT

EXECUTIVE SECRETARY

WILLIAM N. CAREY

ASSISTANT TREASURER

GEORGE W. BURPEE

ASSISTANT SECRETARY

E. L. CHANDLER

PROCEEDINGS OF THE SOCIETY

HAROLD T. LARSEN

Manager of Technical Publications

DEFOREST A. MATTESON, JR.

Editor of Technical Publications

PAUL A. PARISI

Asst. Editor of Technical Publications

COMMITTEE ON PUBLICATIONS

LOUIS R. HOWSON

FRANCIS S. FRIEL

GLENN W. HOLCOMB

I. C. STEELE

FRANK A. MARSTON

NORMAN R. MOORE